Frontiers in Bioscience Scholar

*Front. Biosci. (Schol Ed)* **2022**; 14(1): 007
https://doi.org/10.31083/j.fbs1401007

*Review*

# Role of Cardiac Magnetic Resonance in the Diagnosis of Infiltrative, Hypertrophic, and Arrhythmogenic Cardiomyopathies

Pedro Carvalho Almeida[1,*,†], Vanessa Lopes[2,†], Luís Amaral Ferreira[1], Nádia Moreira[2], Carlos Miguel Marto[3,4,5,6,7], Lino Gonçalves[2,5,6,7,8], Paulo Donato[1,7]

[1]Medical Imaging Department, Coimbra Hospital and University Center, 3000-075 Coimbra, Portugal
[2]Cardiology Department, Coimbra Hospital and University Center, 3000-075 Coimbra, Portugal
[3]Institute of Experimental Pathology, Faculty of Medicine, University of Coimbra, 3000-548 Coimbra, Portugal
[4]Institute for Clinical and Biomedical Research (iCBR), Area of Environment, Genetics and Oncobiology (CIMAGO), Faculty of Medicine, University of Coimbra, 3000-548 Coimbra, Portugal
[5]Center for Innovative Biomedicine and Biotechnology (CIBB), University of Coimbra, 3000-548 Coimbra, Portugal
[6]Clinical Academic Center of Coimbra (CACC), 3000-075 Coimbra, Portugal
[7]Faculty of Medicine, University of Coimbra, 3000-548 Coimbra, Portugal
[8]Institute for Clinical and Biomedical Research (iCBR), Faculty of Medicine, University of Coimbra, 3000-548 Coimbra, Portugal
*Correspondence: pedroalmeida.pmca@gmail.com (Pedro Carvalho Almeida)
[†]These authors contributed equally.

Academic Editor: Gustavo Caetano-Anollés
Submitted: 24 December 2021 Revised: 12 February 2022 Accepted: 22 February 2022 Published: 8 March 2022

**Abstract**

Cardiac magnetic resonance has become a reliable imaging modality providing structural and functional data, and fundamental information about tissue composition. Cardiac magnetic resonance imaging with late gadolinium enhancement, T1-mapping, T2-mapping, T2*-imaging, and extracellular volume, has proved to be a valuable tool in investigating the etiology of heart failure. Such analysis is helpful for the diagnostic evaluation of both ischemic and non-ischemic cardiomyopathies. As primary heart muscle diseases, the ability to characterize the myocardial substrate is essential. Determining the heart failure etiology is fundamental and has implications regarding the prognosis prediction and best treatment. Investigation in cardiac magnetic resonance in heart failure patients has grown in the past decade, and the true value of this imaging modality to detect early disease likely remains underestimated. This review describes the importance of cardiac magnetic resonance for the diagnosis and prognosis of non-ischemic cardiomyopathies, particularly hypertrophic, infiltrative, and arrhythmogenic cardiomyopathies.

**Keywords:** cardiac magnetic resonance; heart failure; cardiomyopathies; myocardium; late gadolinium enhancement; T1 mapping; hypertrophic cardiomyopathy; amyloidosis; arrhythmogenic cardiomyopathy

## 1. Introduction

Lately, cardiac magnetic resonance (CMR) has emerged as a reliable imaging modality providing functional and structural data, and fundamental information regarding tissue composition [1]. CMR of the myocardium is based on different tissues' intrinsic magnetic properties (T1, T2, and T2*). Late gadolinium enhancement (LGE) technique and calculation of extracellular volume (ECV) are examples where the administration of a contrast agent enhances the referred intrinsic magnetic properties [1,2]. Such analysis is useful in assessing patients with heart failure (HF) for the diagnostic evaluation of ischemic and non-ischemic cardiomyopathies.

Establishing the etiology of HF is clinically important, as it has implications for the optimal treatment strategy and prognosis prediction [3]. Echocardiography is fundamental for diagnosing non-ischemic cardiomyopathies, but CMR provides more accurate morphological and prognostic information. In fact, the most recent 2021 European Society of Cardiology (ESC) HF guideline recommends CMR for tissue characterization in the initial assessment of patients with HF and suspected cardiomyopathy [4].

This review describes the importance of CMR for the diagnosis and prognosis of non-ischemic cardiomyopathies, particularly of hypertrophic, infiltrative, and arrhythmogenic cardiomyopathies.

## 2. Hypertrophic Cardiomyopathy

Hypertrophic cardiomyopathy (HCM) is the most prevalent genetically determined heart disorder, affecting 1 in 200 to 500 persons [5,6]. The disease is characterized by an increase of left ventricular (LV) wall thickness (maximal end-diastolic wall thickness of $\geq$15 mm) with a non-dilated LV chamber without any detectable cardiac, systemic, or metabolic disease [7,8]. When a family history of HCM or a positive genetic test for sarcomeric proteins mutations are present, more limited hypertrophy (13–14 mm) may be diagnostic [8].

The clinical presentation is variable. While several patients with HCM are asymptomatic, others may present with palpitations, syncope, exertional dyspnea, or chest pain [9]. Rare cases with HCM present with sudden cardiac death (SCD) as their first clinical symptom, most commonly because of ventricular arrhythmias [10].

Transthoracic echocardiography remains the imaging technique of choice for the initial and successive evaluation of HCM in most patients [8]. Recently, CMR arised as a robust complementary tool, capable of providing information on cardiac phenotypic expression, its hemodynamic and functional characterization, microvascular dysfunction, and myocardial fibrosis [7,11]. Compared with CMR imaging, echocardiography may overestimate the maximal LV wall thickness measurements, particularly when muscle structures of the right ventricle (RV), such as *crista supraventricularis*, are included [12]. Contrastingly, LV wall thickness measurements can be underestimated by echocardiography, especially when hypertrophy is limited to the anterolateral free wall, posterior septum, or apex [13]. CMR is more sensitive to detect left ventricular hypertrophy (LVH) due to its enhanced spatial resolution, allowing a better contrast between the dark myocardium and the bright blood. Additionally, it lacks the limitations of either poor acoustic windows or imaging planes [11,14]. These reasons, ultimately support the role of multiparametric CMR in providing exceedingly accurate measurements of end-diastolic LV wall thickness, LV mass and systolic function, quantification of LV and RV chamber size, and identifying LVH areas which are less reliably detected by echocardiography [5,8,14,15].

### *2.1 Phenotypic Expression*

The distribution of LVH in most patients is asymmetric and often separated by areas of normal wall thickness, providing a non-contiguous pattern [14]. The anterior free wall and contiguous basal anterior ventricular septum are the most common location of LVH (Fig. 1) [13]. In a small subset of patients, the LVH is only confined to one or two LV segments, which can explain why nearly 20% of HCM patients have normal LV mass index values in CMR [13,16]. Patients with a LV wall thickness $\geq$30 mm represent a subgroup at risk for progressive drug-refractory HF secondary to left ventricular outflow tract (LVOT) obstruction and arrhythmic sudden death [17,18].

The second most common phenotype is concentric HCM, characterized by global thickening of the LV with no regional preferences and reduced LV cavity dimensions [19]. Differentiating concentric HCM from acquired causes of concentric LVH, like aortic stenosis, hypertension, or athlete's heart, is frequently challenging. Aortic stenosis can be ruled out by echocardiography in most cases. In complex cases, to obtain a more precise measurement of the aortic valve area and the transvalvular pressure gradient, cine imaging and velocity-encoded imaging can be combined [20]. In hypertensive heart disease with LV wall hypertrophy $\geq$15 mm, the presence of an elevated indexed LV mass, the lack of both mid-wall LGE and systolic anterior motion (SAM) of the mitral valve are significant disease predictors [21]. Also, the native T1 value is an independent discriminator between HCM and hypertensive heart disease [22]. Regarding athlete's heart, LVH rarely exceeds 16 mm, LV cavity size is normal or enlarged, and there is no evidence of diastolic dysfunction nor extensive LGE despite LV remodeling [11,19]. Regression in LV wall thickness after a period of systemic deconditioning is expected in an athlete's heart [15].

Other infiltrative diseases such as cardiac amyloidosis (CA), Anderson-Fabry disease (AFD), or iron overload cardiomyopathy (IOC) can also manifest as diffuse myocardial hypertrophy as discussed later in this review.

Further phenotypic variations occur, such as midventricular HCM (involvement of midseptum and free wall) and apical HCM (wall thickening confined to the apex and the distinctive "ace of spades" configuration at end-diastole in CMR) [15]. Occasionally, these patients develop a dyskinetic or akinetic apical aneurysm. These features are linked to a higher risk of arrhythmic sudden death and thromboembolic events [23,24]. Intracardiac thrombus, if present, appears as a low-signal intensity mass distinguishable from surrounding high-intensity structures in contrast-enhanced CMR (Fig. 2) [25]. Since echocardiography can be suboptimal in evaluating the apex, CMR plays an important role depicting apical hypertrophy, apical akinesis, and small-to-moderately sized apical aneurysms [26].

Even though HCM is classically a disease of the LV, several patients with HCM have RV hypertrophy and/or dysfunction; therefore, RV assessment should be included in the imaging workup of these patients [27].

Some morphological abnormalities in genetic carriers without LVH, like myocardial crypts (blood-filled fissures in the myocardium of LV), have been described as a subtle marker of HCM [28,29]. However, recent reports have supported the hypothesis that crypts are benign anatomical variants, frequent in healthy subjects, and not connected to major adverse cardiovascular events [30].

A minority of HCM patients develop the so-called end-stage phase of the disease, with regression of hypertrophied and hypercontractile non-dilated LV to severe systolic dysfunction (ejection fraction $<$50%), enlarged ventricular chambers, increased end-diastolic and end-systolic volumes, defined as LV remodeling [31].

Apart from the presence of LVH, other structural manifestations of HCM include left atrial remodeling, myocardial bridging of coronary arteries, microvascular dysfunction, myocardial fibrosis, areas of LV noncompaction, LVOT obstruction, and abnormalities of papillary muscles and mitral apparatus [7].

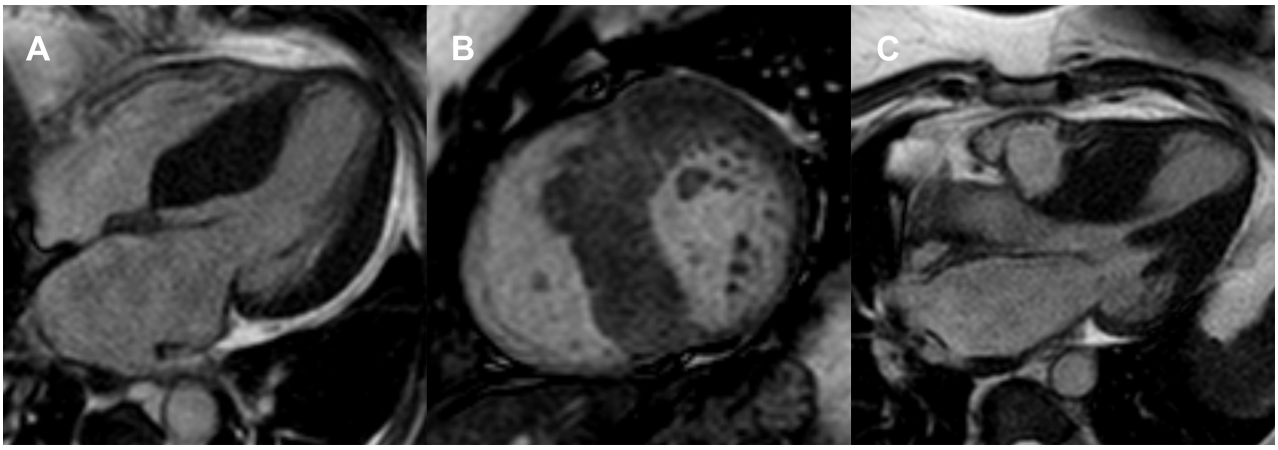


**Fig. 1. Asymmetric septal nonobstructive hypertrophic cardiomyopathy (HCM).** Steady-state free precession (SSFP) magnetic resonance images of a patient with a maximal left ventricular wall thickness of 31 mm in the mid inferoseptal are shown (A) in horizontal long-axis, (B) in midventricular short-axis, and (C) along the left ventricular outflow tract (LVOT).

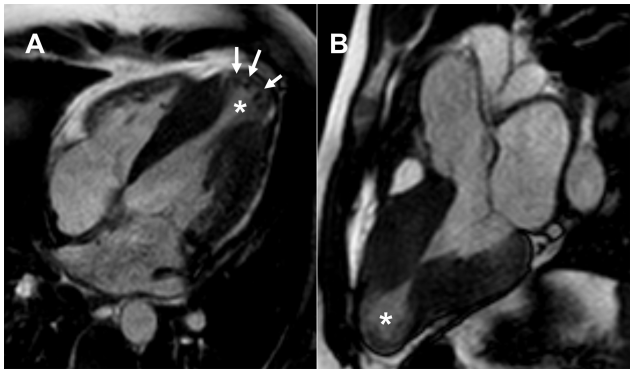


**Fig. 2. Midventricular hypertrophic cardiomyopathy (HCM).** Steady-state free precession (SSFP) magnetic resonance images are shown (A) in horizontal long-axis and (B) along the left ventricular outflow tract (LVOT), depicting apical aneurysm (asterisk) and millimetric intracardiac thrombus within the aneurysm (white arrows).

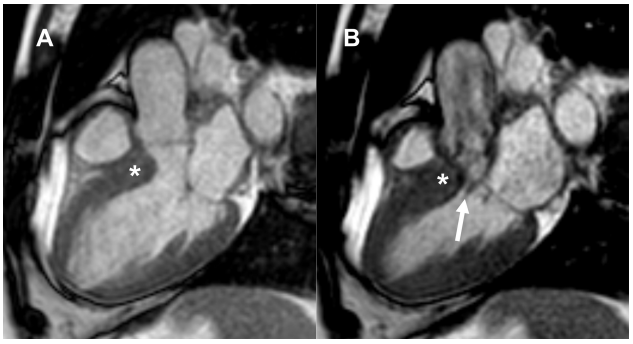


**Fig. 3. Asymmetric septal obstructive hypertrophic cardiomyopathy (HCM).** Longitudinal cine steady-state free precession (SSFP) magnetic resonance images through left ventricular outflow tract (LVOT) at (A) end-diastole and (B) early systole depicting systolic anterior motion (SAM) of anterior mitral valve leaflet (white arrow) and thickened ventricular septum (asterisk).

### *2.2 Mitral Valve and Subvalvular Apparatus*

Around 70% of patients with HCM present with LVOT obstruction (gradient $\geq$30 mmHg) at rest or with provocative maneuvers [32]. Mitral valve and subvalvular apparatus morphologic and functional abnormalities contribute to LVOT obstruction, and the diagnosis of these findings may dictate a specific management strategy [33–35]. Abnormal acceleration and misdirection of the flow toward the LVOT during systole create a drag effect pushing the mitral leaflets anteriorly, also known as SAM. It causes septal contact, flow resistance, and incompletely coaptation of anterior and posterior leaflets leading to mitral regurgitation [36]. CMR imaging using perpendicular and longitudinal cine sequences through the LVOT allows excellent depiction of the SAM and the signal void caused by high-velocity jet across the LVOT as well as mitral regurgitation (Fig. 3) [7,15].

Regarding structural abnormalities of the mitral valve, the most frequent is the marked elongation of both mitral leaflets [33]. Subvalvular abnormalities include hypertrophy and variation of the papillary muscle (PM) morphology (double bifid PM and anteroapical displacement of the anterolateral PM), which may also contribute to the severity of LVOT obstruction by anteriorly displacing the mitral valve plane toward the interventricular septum [37,38].

### *2.3 Late Gadolinium Enhancement*

Late gadolinium enhancement depends on varying uptake and washout patterns between normal and abnormal myocardium [39]. Following intravenous administration, gadolinium-based contrast agents accumulate in areas with expanded extracellular space due to either necrotic myocardium or scar tissue, resulting in increased signal intensity on T1-weighted gradient echo sequences [40]. This is depicted by applying an inversion recovery preparation

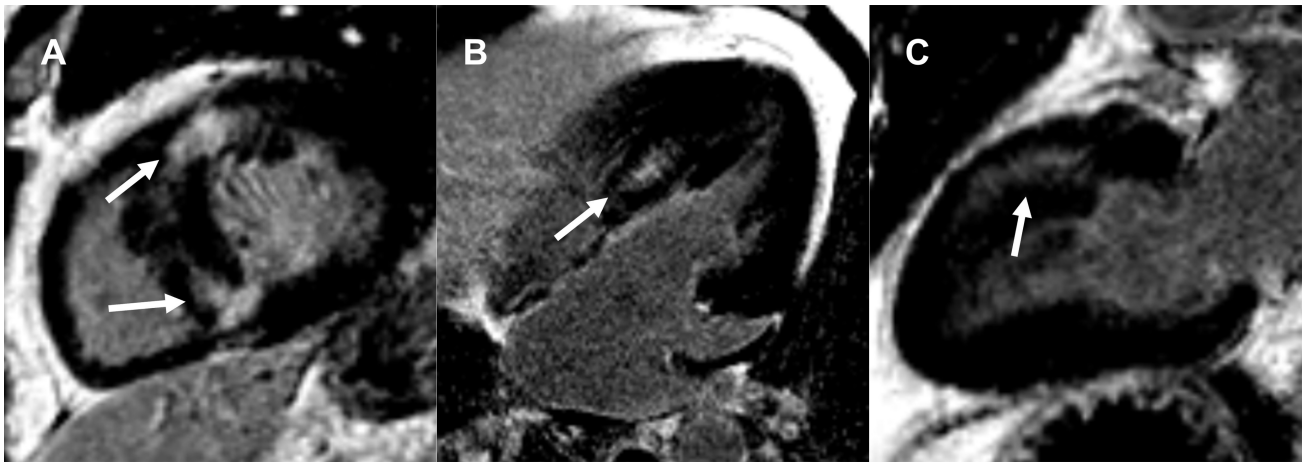


**Fig. 4. Late gadolinium enhancement (LGE) in hypertrophic cardiomyopathy (HCM).** (A) Short axis view with hyperenhancement (white arrows) at the right ventricular insertion to the ventricular septum. (B) Horizontal long-axis view and (C) vertical long-axis view show a patchy mid-wall hyperenhancement (white arrows) in the hypertrophic segments.

pulse to achieve myocardial signal nulling while the scar tissue and blood remain bright [41].

The prevalence of LGE in patients with HCM is 60% [42]. It is well established that LGE is a noninvasive marker of increased risk for ventricular arrhythmias and HF progression with systolic dysfunction [42–45]. The most common pattern or distribution of LGE in HCM is a punctuate and/or patchy mid-wall hyperenhancement at a non-coronary vascular distribution in the hypertrophic segments (Fig. 4), although HCM may present practically with any pattern [19]. The extent of LGE appears to have more discriminatory value than its presence, in particular when LGE is $\geq$15% of the LV mass, which demonstrated a significant increase in SCD risk [46]. However, LGE may also be found in hearts with no histopathological evidence of microvascular ischemia, mainly when circumscribed to areas of RV insertion to the ventricular septum. It is believed that these areas represent an expanded extracellular matrix created by the confluence of intersecting myofibrils [47].

Some limitations to this technique have been reported, especially when diffuse myocardial fibrosis is present and the myocardial signal intensity is nearly isointense and in patients with subtle diffuse enhancement [48,49]. T1 mapping is a novel and robust CMR technique, which offers quantitative measures of the myocardial signal. It creates a pixel-wise parametric map, in which each pixel reflects the absolute value of T1, coded in color (Fig. 5) [50]. Moreover, it directly measures ECV fraction from T1 values before (native T1) and after administration of gadolinium [14]. Increased native myocardial T1 values and an elevated ECV fraction were found in HCM, even in non-hypertrophic segments with preserved contraction function or in patients without LGE, suggesting that myocardial tissue remodeling may precede morphological and functional changes [49,51].

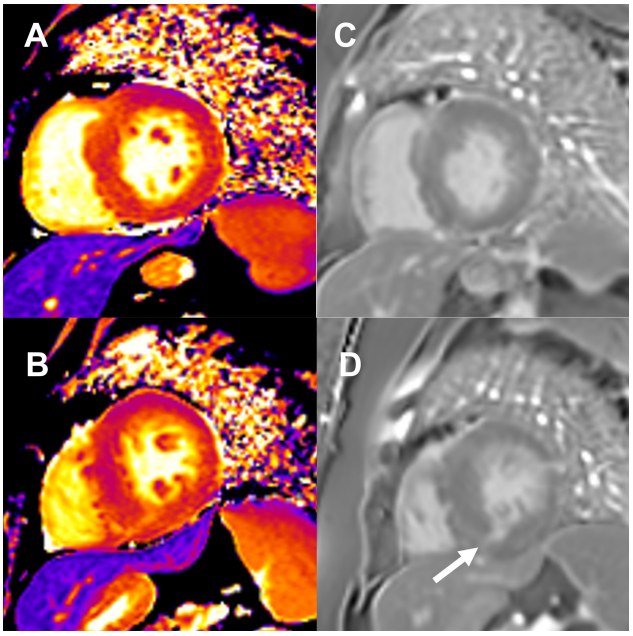


**Fig. 5. Native T1 mapping and late gadolinium enhancement (LGE) images in hypertrophic cardiomyopathy (HCM).** Native T1 mapping with high signal at (A) mid-septal wall and (B) mid inferoseptal segment (white arrow). (C,D) Corresponding phase-sensitive inversion recovery (PSIR) imaging shows late gadolinium enhancement in the same regions.

### *2.4 SCD Risk Assessment and Implantable Cardioverter-Defibrillator (ICD) Decision-Making*

Besides diagnosis, phenotypic characterization, and planning for septal reduction procedures, CMR is also increasingly important for risk stratification and prognosis in HCM. According to the 2020 American Heart Association (AHA)/American College of Cardiology (ACC) guideline for the diagnosis and treatment of patients with HCM [8],

CMR plays a crucial role in the risk stratification and subsequent decision to ICD placement. On the contrary, the ESC guideline does not endorse LGE for risk stratification purposes and continues to recommend the HCM Risk-SCD score, despite debate on the value of the latter approach [28,52,53]. CMR allows assessment of maximum LV wall thickness, LV ejection fraction, LV apical aneurysm, and extent of myocardial fibrosis with LGE, all of which are used in ICD decision-making [8]. Massive LVH and systolic dysfunction (ejection fraction $<$50%) are common indications for ICD placement, being CMR the gold standard to measure ventricular wall thickness and function [8]. Apical aneurysms, which echocardiography may fail to detect, are also better assessed with CMR [24].

As stated above, the extent of scar, imaged by LGE is associated with increased risk for potentially life-threatening ventricular arrhythmias and cardiac death [46,54,55]. Based on this evidence, the AHA/ACC guideline recommends ICD placement in the presence of extensive LGE ($\geq$15% of LV mass) (2b recommendation) [8]. Further randomized trials are needed to confirm and assess the value of CMR for SCD risk stratification in HCM.

## 3. Infiltrative Cardiomyopathies

Infiltrative cardiomyopathies refer to deposits of substances in the myocardial tissue resulting in a structural abnormality and/or alteration of cardiac function. They include CA, IOC, AFD, Danon disease, Friedreich's Ataxia, and other rare conditions [56]. In this review we will focus on the most common infiltrative cardiomyopathies: CA, IOC, and AFD.

### *3.1 Cardiac Amyloidosis*

Systemic amyloidosis comprises a group of diseases caused by the deposition of insoluble amyloid fibrils in the extracellular space of tissues and organs. This deposition ultimately leads to progressive organ failure [57]. CA is an infiltrative cardiomyopathy characterized by increased biventricular wall thickening, restrictive LV filling, and, frequently, a non-dilated LV cavity with preserved or mildly depressed LV systolic function [58]. Previously thought to be rare, CA is now understood to be underdiagnosed [59].

Most cases of cardiac involvement occur in two types of amyloidosis: light chain immunoglobulin (AL) and transthyretin amyloidosis (ATTR). ATTR is further classified into the wild-type ($>$90% of cases) and hereditary ($<$10% of cases) [4]. The main treatment options in AL-CA are chemotherapy or autologous stem-cell transplant, aimed at the underlying hematological condition. Treatment of ATTR is mainly based on stabilization and reduction of transthyretin production. Liver and/or cardiac transplantation can be considered only in end-stage disease of familial ATTR [4]. Tafamidis showed reduction of all-cause mortality and cardiovascular hospitalizations in hereditary and wild-type ATTR, mostly in those patients with New York Heart Association (NYHA) class I and II at baseline [60].

Echocardiography is often the first imaging modality performed in patients presenting with HF. CA's echocardiographic features are frequently present in patients with advanced disease but absent earlier [61]. In recent years, the application of CMR in CA has increased, since it provides information regarding the presence, distribution, and location of hypertrophy, visualization of cardiac amyloid infiltration with LGE imaging, and measurement of cardiac amyloid burden with T1 mapping and ECV [62–64]. Additionally, CMR findings appear to have prognostic significance [65]. Technical development of new CMR sequences has contributed to CA awareness and recognition [1]. Furthermore, the emergence of new treatment strategies for CA, such as tafamidis, entails a need to establish the diagnosis during the earlier stages of the disease to prolong survival and improve outcomes.

#### 3.1.1 Cardiac Morphology and Function

Extracellular deposition of amyloid protein in CA produces an appearance of hypertrophy with non-dilated or small ventricles [66]. The pattern of hypertrophy can be asymmetric or symmetric, eccentric or concentric [66]. Among patients with ATTR, the most common morphological phenotype is asymmetrical LVH (ratio between the septal and posterior wall $>$1.5), found in 79% of patients [67]. Asymmetrical septal hypertrophy can present as sigmoid septum (found in 55% of patients with ATTR) or reverse septal contour (24% of patients with ATTR). The wild-type and hereditary ATTR subtypes present no differences in their morphological phenotype [1]. CA's asymmetric septal hypertrophy pattern can be mistaken for HCM; therefore, its presence should be interpreted with caution. CMR is effective to differentiate CA from HCM and hypertensive heart disease, and LGE images can readily differentiate these conditions [58,66,68,69]. In AL-CA, symmetrical and concentric LVH was the most common pattern, present in 68% of patients [70].

Cardiac magnetic resonance can qualitative and quantitatively assess global and regional LV systolic function. Cardiac amyloid infiltration results in low end-diastolic volume, diastolic dysfunction, restrictive physiology with late depressed systolic function, arrhythmias, and HF [68]. The most recent 2021 ESC HF guidelines [4] state that CA should be suspected in any patient who presents with HF and preserved LV ejection fraction. The apical function is preserved until late, a typical pattern known as "apical sparing" [66]. Right ventricular and papillary muscle hypertrophy, biatrial dilation, thickening of the interatrial septum, valve leaflet thickening, and pericardial effusion are also frequently found [1].

#### 3.1.2 Late Gadolinium Enhancement

In CA, there is an expansion of the extracellular space due to increased amyloid deposition, leading to high

gadolinium concentrations in the myocardium and prolonged impermeability, resulting in LGE [70,71]. LGE imaging provides highly characteristic findings with high diagnostic accuracy [72]. CA presents a distinctive pattern of LGE with global subendocardial or transmural distribution, associated with dark blood-pool due to abnormal gadolinium kinetics [73]. Three LGE patterns were identified in CA: none, subendocardial and transmural (Fig. 6). These patterns are a continuum and correlate with the extent of myocardial infiltration [74]. Transmural LGE is associated with the highest amyloid infiltration in advanced CA and has shown to carry the most adverse prognosis [74]. As opposed to myocardial infarction, LGE in CA is not limited to characteristic vascular territories nor is sharply defined [75]. RV LGE is also frequently present [67]. LGE is present in most cases of CA (100% LGE in LV and 96% in RV), being more common in ATTR (vs. AL-CA), but does not differentiate between CA subtypes [67].

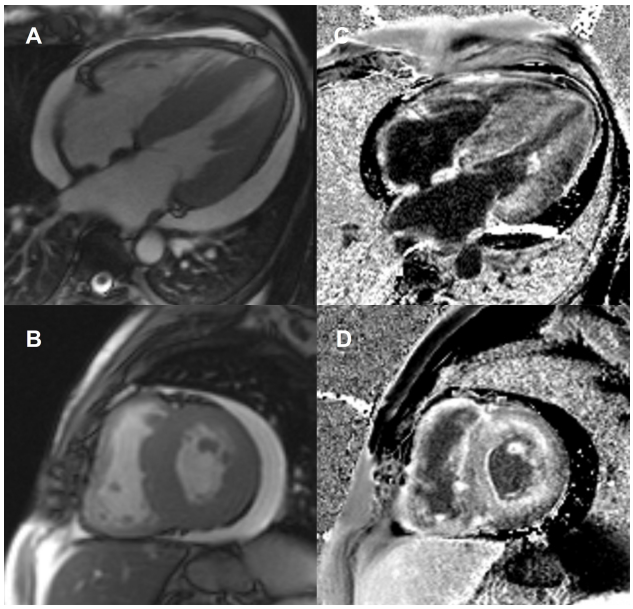


**Fig. 6. Cardiac amyloidosis.** Steady-state free precession (SSFP) magnetic resonance images at (A) end-diastolic horizontal long-axis and (B) midventricular short-axis showing concentric thickening of left ventricular walls (septal wall measuring 26 mm), right ventricular thickening, biatrial dilatation, interatrial septal thickening (9 mm), and pericardial effusion. The corresponding late gadolinium enhancement (LGE) images (C and D) show extensive amyloid infiltration with generalized gadolinium uptake.

As previously stated, traditional LGE imaging is a comparison technique, based on differences between normal and abnormal myocardium. The null inversion time is chosen based on what the operator considers normal myocardium. By convention, the areas with the most contrast concentration should have a brighter display, and normal myocardium should be presented as black or "nulled" on LGE imaging. Nulling the normal myocardium in diffuse infiltrative diseases such as CA can be challenging given the lack of normal myocardium areas for comparison. The myocardial signal intensity may be globally "nulled," thus looking like normal tissue [1,67]. It is a clear indication of the presence of amyloidosis when achieving the usual contrasts in LGE imaging is a challenging task [75]. More recent techniques, such as phase-sensitive inversion recovery (PSIR), are less operator-dependent and more precise in defining the degree of cardiac involvement. A combination of LGE with T1 mapping is another alternative to address this issue [1,72,74].

Other limitations of LGE include the use of gadolinium which is relatively contraindicated in patients with severe renal dysfunction, common in patients with amyloid disease, and lack of quantitative results, limiting the ability to track changes over time. However, T1 mapping can overcome these limitations and potentially detect amyloid infiltration at an earlier stage of the disease than LGE [61,76].

### 3.1.3 T1 Mapping

In CA, native myocardial T1 is significantly increased, and ECV expanded, with corresponding extensive LGE [77]. In a study of 868 patients with suspected CA, T1 mapping diagnosed CA with a sensitivity of 85% and specificity of 87% [78]. Importantly, native myocardial T1 elevation is also an early disease marker [64]. It increases with cardiac amyloid infiltration and correlates with markers of systolic and diastolic dysfunction [63]. T1 mapping can also measure the continuum of cardiac amyloid infiltration from early stages to diffuse transmural involvement [57]. Native T1 values over 1136 ms strongly suggest cardiac amyloid in patients with a clinical suspicion [78]. A CMR algorithm to minimize the use of contrast to evaluate patients with suspected amyloidosis has been proposed [78]. Native myocardial T1 mapping detects both ATTR and AL-CA with similar diagnostic accuracy, but ATTR presents lower maximal T1 elevation [64].

Native T1 mapping waives the use of gadolinium, playing an advantage to LGE [78]. However, native T1 measures myocardial signal from both the interstitium and cardiomyocytes, without distinguishing between the underlying processes (fibrosis, edema, amyloid, myocyte volume) [1]. A signal from the interstitium alone is somewhat diluted by the myocyte signal, so subtle differences are more difficult to detect. Moreover, capillary density, capillary vasodilatation, and "partial voluming" between blood pool and myocardium are also measured [79,80]. The use of gadolinium and ECV measurements allow the isolation of the signal from the extracellular space [1]. Therefore, ECV is a more reliable marker of amyloid infiltration [57].

### 3.1.4 Extracellular Volume Fraction Measurement

Post-contrast T1 is dominated by, and inversely proportional to, the gadolinium concentration in tissue. Mea-

suring T1 after contrast provides a value linked to the interstitium. Post-contrast T1 value changes with gadolinium dose, post bolus time, and patient-specific factors, such as hematocrit, limiting its evaluation of the myocardium separately [66,79]. If T1 is measured before and after contrast, adjusted for hematocrit, the extracellular space signal can be isolated with the measurement of the ECV [66]. The myocardial ECV represents the proportion of extracellular water, a proxy for the process of holding water, be it fibrosis, amyloid, or edema [79]. In CA, ECV values are markedly elevated and tend to be higher than in any other cardiomyopathy [63–65]. ECV allows a noninvasive quantification of the cardiac amyloid burden. Its elevation during cardiac infiltration may be detected early before developing LVH, LGE, or elevation in serum biomarkers, suggesting that ECV is a marker of early disease [62]. Furthermore, ECV predicts mortality in ATTR. Both native T1 and ECV predicted survival in ATTR; however, ECV is a more robust predictor [57,67]. ECV appears to be greater in ATTR [57,74] but does not seem to differentiate between the subtypes of CA [62].

#### 3.1.5 T2-weighted CMR

T2-weighted CMR can detect myocardial edema, which is present in CA. There has not been as extensive evaluation of parametric sequences to measure myocardial T2 relaxation in CA when compared with native T1 values or ECV [61]. In a recent study, T2 was found to be higher in untreated AL-CA than treated AL-CA and ATTR, and predicts prognosis in AL-CA [81].

### *3.2 Iron Overload Cardiomyopathy*

Iron overload is a systemic process characterized by an increased level of plasma iron and iron accumulation in parenchymal cells [82]. Its detection is imperative owing to multisystem manifestation such as myocardial disease, type 2 diabetes mellitus, or liver cirrhosis with increased risk of hepatocellular carcinoma [82]. IOC describes the different forms of cardiac dysfunction in the setting of increased gastrointestinal iron absorption (e.g., hereditary hemochromatosis) or as a result of transfusion-dependent anemias (e.g., thalassemia major and sickle cell disease) [83]. Early stages of IOC present as restrictive cardiomyopathy with diastolic LV dysfunction. If iron overload persists and no proper therapy is started, dilated cardiomyopathy with chamber dilatation and impaired systolic function may develop [84].

Cardiac magnetic resonance is the only non-invasive technique for quantifying myocardial iron overload (MIO). It is considered the standard of care in diagnosing and monitoring iron overload diseases [85,86]. The presence of myocardial iron deposits causes magnetic field inhomogeneity and accelerates the relaxation times [87,88]. As the myocardial iron concentration increases, the signal intensity in T1-, T2- and T2*- weighted images decreases [89,90]. CMR gradient-echo T2* relaxation time is currently the mainstay of IOC diagnosis, and the measure in a single slice of a full-thickness region of interest in the mid-ventricular septum is highly representative of global myocardial iron distribution [83,91]. A multislice segmental approach is also validated and allows the identification of different patterns of iron distribution (homogenous MIO, heterogeneous MIO, and no MIO) that correlate with cardiac complications [92,93]. A cardiac T2* relaxation time of $<$20 ms has been proposed as a cutoff value for diagnosing MIO and substantially better predictor for HF (T2* $<$10 ms) and arrhythmias (T2* $<$20 ms) than liver T2* or serum ferritin [94]. This non-invasive modality is also helpful in identifying the proper moment to initiate therapy and monitor therapy response by serial imaging, which has a significant positive impact on the survival of these patients [91,95].

### *3.3 Anderson-Fabry Disease*

Anderson-Fabry disease is an X-linked congenital error of the glycosphingolipid metabolic pathway due to the absent or deficient activity of $\alpha$-galactosidase A ($\alpha$-Gal A) enzyme and is the most prevalent lysosomal storage disorder [96]. It results in a progressive glycosphingolipid accumulation within lysosomes in multiple cell types, including capillary endothelial, renal, nerve, and cardiac cells [97]. In adulthood, progressive cardiovascular involvement and renal failure account for most deaths associated with the disease [98]. Over 60% of patients present with cardiovascular signs such as arrhythmias and conduction abnormalities, aortic and mitral valves deformities, LV mild-to-moderate concentric hypertrophy, and HF [99,100]. Since treatment with enzyme replacement therapy has been shown to reverse or slow disease progression, early diagnosis is critical, and CMR plays an important role in this field [100].

Non-invasive detection and monitoring of cardiovascular manifestations of AFD have focused on LVH, the classical morphological abnormality of the disease, which can mimic the HCM. In fact, the prevalence of AFD gene mutations in patients with unexplained LVH is 0.5% [101]. LV concentric thickening is the most common morphological manifestation of AFD, but the spectrum also includes apical and asymmetric septal hypertrophy [102]. CMR imaging allows improved visualization of LV geometry and identification of hypertrophy, particularly in segments not well characterized by echocardiography, and quantification of LV mass index [103,104]. Due to its higher precision, CMR has also been proposed for LVH follow-up and response monitoring of patients treated with enzyme replacement therapy [100,104].

LGE is identified in up to 50% of AFD patients in the basal and/or mid inferolateral wall, with a mid-myocardial pattern [99,105,106]. The presence and extent of LGE are associated with a greater risk of adverse cardiac events, such as ventricular arrhythmias and SCD [102,107]. Unfortunately, it is known that LGE imaging is less sensitive

in the setting of a diffuse process, and the advanced renal dysfunction of some of these patients often precludes the use of contrast [40].

Tissue characterization using T1 mapping is a powerful tool in diagnosing cardiac involvement in AFD since the sphingolipid deposition in the myocardium provides a low native T1 value allowing distinction from other causes of LVH, which generally have an elevated T1 [108,109]. It has been reported that in AFD without LVH or fibrosis, native T1 values may still be lower than normal, suggesting that it could be used as an early marker of cardiac involvement and a prompt the initiation of ERT to achieve long-term improvements [108,110]. Furthermore, compared with healthy controls, these patients present normal myocardial ECV, suggesting no diffuse fibrosis [106,109].

## 4. Arrhythmogenic Cardiomyopathy

Arrhythmogenic cardiomyopathy (AC) is an inherited heart muscle disease characterized macroscopically by fibrofatty replacement of the RV myocardium, that may predispose to ventricular arrhythmias, unexplained syncope, and/or SCD. Therefore, an accurate and early diagnosis of AC is critical [111,112]. The classic AC phenotype is characterized by isolated RV involvement, thus previously being designated arrhythmogenic right ventricular cardiomyopathy. More recently, genotype/phenotype studies have shown that biventricular and left-dominant disease variants are frequent and have led to the use of the term AC [4,111].

Because the diagnosis of AC is challenging, an International Task Force (ITF) developed criteria, which were revised in 2010 [113]. ITF criteria for the diagnosis of AC are based on several parameters, including: global or regional dysfunction and structural alteration of the RV demonstrated on imaging; tissue characterization by endomyocardial biopsy; repolarization and depolarization electrocardiographic abnormalities; arrhythmias; and family history [113]. Therefore, AC diagnosis cannot be made based on imaging alone.

CMR examination is part of the criteria for the qualitative assessment of regional RV wall motion abnormality on cine images (RV regional akinesia, dyskinesia, dyssynchrony), combined with quantitative assessment of RV dilatation or global RV systolic dysfunction. CMR major criteria require regional RV wall motion abnormality (akinesis or dyskinesis or dyssynchronous RV contraction) and either increased RV end-diastolic volume ($\geq$110 mL/m$^2$ in men; $\geq$100 mL/m$^2$ in women) or depressed RV ejection fraction (RV ejection fraction $\leq$40%). Minor criteria on CMR requires regional RV wall motion abnormality (as mentioned before) and milder degrees of RV end-diastolic volume dilation ($\geq$100 mL/m$^2$ in men; $\geq$90 mL/m$^2$in women) or RV ejection fraction $\leq$45% [113].

The revised ITF criteria did not include contrast-enhanced CMR, even being the only imaging modality able to identify fatty tissue on spin-echo sequences and fibrosis as LGE deposition [114]. Difficulty in the interpretation, limited experience, and low specificity of tissue characterization findings by CMR were among the reasons not to be included [113].

However, in recent years, CMR has emerged as the primary imaging modality in AC, since it allows for non-invasive multiplane morphologic and functional evaluation, and tissue characterization [114,115]. CMR is the recommended modality for establishing a diagnosis of AC and adequate characterization of the disease phenotypic variant [111].

### *4.1 Regional Systolic Wall Motion Abnormalities*

In AC, CMR may reveal global and regional ventricular dilation, global ventricular dysfunction, and regional wall motion abnormalities (Fig. 7). Regional wall motion abnormalities occur preferentially in the subtricuspid region. The “accordion sign”, that represents a focal “crinkling” of the myocardium, is an example of these abnormalities, which is caused by a small region with dyssynchronous contraction [112].

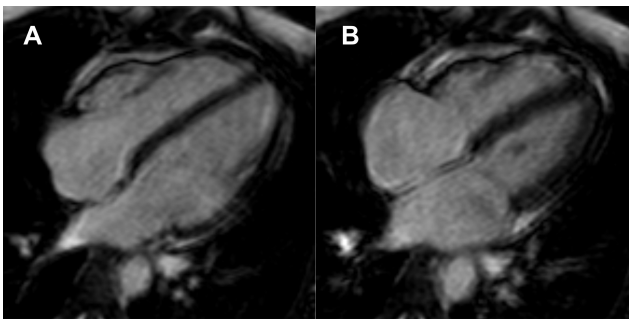


**Fig. 7. Arrhythmogenic cardiomyopathy with isolated right ventricular involvement.** Steady-state free precession (SSFP) magnetic resonance images at (A) end-diastolic and (B) end-systolic horizontal long-axis shows dilated right ventricle with mild-moderately depressed systolic function, akinesia/mild dyskinesia of the basal segment of the right ventricle free wall; and mild right atrial dilatation. Left ventricle morphology and systolic function are within the normal range.

Nearly all patients with AC (96% of patients) present an abnormal RV on CMR [116]. The most frequent RV abnormalities are basal inferior wall dyskinesia (in 94% of cases) and basal anterior wall dyskinesia (87% of cases). Although clinical studies have focused predominantly on RV abnormalities, LV involvement is more common than previously thought. LV involvement occurs in 52% of patients, which has led to the reconsideration of the initial dysplasia triangle (posterior lateral wall of the LV, subtricuspid, and anterior wall of the RV) [116]. Clinically demonstrable RV involvement in biventricular variants of AC is

**Table 1. Cardiac magnetic resonance main findings in non-ischemic cardiomyopathies.**

| Condition | Main CMR findings | Markers of worse prognosis in CMR |
|---|---|---|
| HCM | Asymmetric septal wall thickening >15 mm<br>Diffuse, mid-cavity, and apical variants | LGE ≥15% of the LV mass |
| | Elongated leaflets of mitral valve and abnormal papillary muscles | |
| | Patchy mid-myocardial LGE in hypertrophied areas<br>Mildly elevated T1 and ECV | LV wall thickness ≥30 mm |
| CA | Biventricular wall thickening with non-dilated ventricles; biatrial dilation; pericardial effusion | LGE |
| | LGE pattern (diffuse, subendocardial, or transmural) | |
| | Markedly elevated native T1 and ECV | Higher ECV fraction |
| | Abnormal gadolinium kinetics | |
| IOC | Cardiac T2* <20 ms | Cardiac T2* <10 ms |
| AFD | LV concentric thickening<br>Patchy mid-myocardial LGE in basal and/or mid inferolateral wall<br>Low native T1 and normal ECV | LGE |
| AC | Global and regional RV dilation and dysfunction<br>Intramyocardial fat<br>LGE<br>Focal wall thinning | Any CMR abnormality |

AC, arrhythmogenic cardiomyopathy; AFD, Anderson-Fabry disease; CA, cardiac amyloidosis; CMR, cardiac magnetic resonance; ECV, extracellular volume; HCM, hypertrophic cardiomyopathy; IOC, iron overload cardiomyopathy; LGE, late gadolinium enhancement; LV, left ventricular; RV, right ventricular.

an important additional criterion to distinguish AC from dilated cardiomyopathy [111].

Cardiac magnetic resonance provides a rigorous quantitative analysis of RV volumes, but significant interobserver variability in the RV free wall segmental contraction analysis and interpretation of qualitative findings have been reported [117]. RV's standardized and regional biventricular analysis using cine steady-state free precession (SSFP) imaging that includes all RV segments may help overcome these limitations [118].

Directly assessing tissue composition of thin RV wall also remains a technical challenge on MRI. Some technical advances may be an encouraging approach to decrease variability in assessing RV function, including semi-automated myocardial deformation quantification, particularly feature tracking [119].

### *4.2 Late Gadolinium Enhancement*

The pathologic hallmark of AC is the fibrofatty replacement of the myocardial tissue. CMR allows tissue characterization (fibrosis, fatty infiltration, and fibrofatty scar), but LGE is not included in the 2010 ITF criteria [113]. The visualization of fat and LGE by CMR as a diagnostic hallmark faces several problems which withheld their use: intramyocardial fat occurs in normal hearts and is not specific for AC without associated functional abnormalities [120]; detection of fibrosis in the RV is nonspecific and frequently difficulted by the thin RV wall, which in AC may be even more pronounced, making the LGE technique less dependable than for the LV [121]; distinguishing fat from fibrosis by LGE sequences is challenging; and finally, LV LGE is nonspecific and has a broad range of differential diagnosis (AC, sarcoidosis, myocarditis, CA, HCM, and dilated cardiomyopathy). The absence of RV myocardial fat in CMR does not exclude the diagnosis of AC, as seen in pediatric patients [117]. The presence of fat should not be interpreted alone [118]. Given the limitations of CMR at evaluation of fat and fibrosis, AC diagnosis is mainly based on establishing the consequence of intramyocardial fibrofatty replacement, such as static morphological abnormalities and regional RV wall motion abnormalities [118].

While these limitations exist, LGE may still be useful in AC evaluation. Diagnostic accuracy for AC was best (98%) when pre-/post-contrast signal abnormalities (including LV fat infiltration and LGE) were considered together with wall motion alterations [122]. LGE may also increase the sensitivity in the diagnosis of biventricular AC by demonstrating segmental subepicardial LGE in the LV wall, which in LV-dominant phenotypic variants of AC may be the only imaging feature [111].

### *4.3 Risk stratification and prognosis*

In patients with suspected AC, a normal CMR had a negative predictive value of 99% for major clinical events in a 4.3-year follow-up, potentially becoming a "rule-out" test for AC [111,123]. Furthermore, no events were observed among patients with a normal CMR during a 6-year follow-up [116]. On the other hand, an abnormal CMR was an independent predictor of events with a cumulative effect of several anomalies (including morphology, wall motion abnormalities, and fat/fibrosis) [123].

CMR has also been useful in the risk stratification for arrhythmic events. In a study with AC mutation carriers, sustained arrhythmias during follow-up were associated with structural abnormalities on CMR [116]. Another study showed that CMR was an independent predictor of ventricular arrhythmias [123]. In patients with AC and ventricular arrhythmias, regional wall-strain assessed on cine-CMR reliably predicts arrhythmogenic ventricular tachycardia-substrate. This technique permits safe and improved diagnostic accuracy in AC, preventing the need for invasive procedures, and facilitates the planning of ventricular tachycardia ablation procedures [124].

Table 1 summarizes the main CMR findings and markers of prognosis in non-ischemic cardiomyopathies.

## 5. Conclusions

Cardiac magnetic resonance imaging with late gadolinium enhancement, T1 mapping, T2 mapping, T2*-imaging, and extracellular volume, has proved to be a valuable tool in investigating the etiology of heart failure. Cardiomyopathies rarely recognized in the past, are now understood to be underdiagnosed, and patients are receiving appropriate treatment thanks to the unparallel capacity of tissue characterization of cardiac magnetic resonance.

Cardiac magnetic resonance findings are proving to be crucial risk markers for prediction of clinical outcomes and can influence clinical management and decision-making in these patients. Therefore, cardiac magnetic resonance is an indispensable imaging modality in determining the diagnosis of nonischemic cardiomyopathies and assessing its prognosis.

## Author contributions

PCA and VL performed the research, analyzed the data, and wrote the original draft. LAF, NM and CMM conceptualized the study, reviewed, and edited the original draft. NM and PD provided scientific support and knowledge. LG and PD provided supervision and critical review of the manuscript. All authors contributed to editorial changes in the manuscript. All authors read and approved the final manuscript.

## Ethics approval and consent to participate

Not applicable.


## Acknowledgment

We acknowledge our hospital colleagues for their help and discussion.

## Funding

This research received no external funding.


## Conflict of interest

The authors declare no conflict of interest.

## References


[1] Martinez-Naharro A, Baksi AJ, Hawkins PN, Fontana M. Diagnostic imaging of cardiac amyloidosis. Nature Reviews Cardiology. 2020; 17: 413–426.

[2] Messroghli DR, Moon JC, Ferreira VM, Grosse-Wortmann L, He T, Kellman P, *et al*. Clinical recommendations for cardiovascular magnetic resonance mapping of T1, T2, T2 and extracellular volume: A consensus statement by the Society for Cardiovascular Magnetic Resonance (SCMR) endorsed by the European Association for Cardiovascular Imagin. Journal of Cardiovascular Magnetic Resonance. 2017; 19: 1–24.

[3] Abbasi SA, Ertel A, Shah RV, Dandekar V, Chung J, Bhat G, *et al*. Impact of cardiovascular magnetic resonance on management and clinical decision-making in heart failure patients. Journal of Cardiovascular Magnetic Resonance. 2013; 15: 89.

[4] McDonagh TA, Metra M, Adamo M, Gardner RS, Baumbach A, Böhm M, *et al*. 2021 ESC Guidelines for the diagnosis and treatment of acute and chronic heart failure. European Heart Journal. 2021; 42: 3599–3726.

[5] Maron BJ. Clinical Course and Management of Hypertrophic Cardiomyopathy. The New England Journal of Medicine. 2018; 379: 655–668.

[6] Geske JB, Ommen SR, Gersh BJ. Hypertrophic Cardiomyopathy: Clinical Update. JACC: Heart Failure. 2018; 6: 364–375.

[7] Bogaert J, Olivotto I. MR Imaging in Hypertrophic Cardiomyopathy: from Magnet to Bedside. Radiology. 2014; 273: 329–348.

[8] Ommen SR, Mital S, Burke MA, Day SM, Deswal A, Elliott P, et al. 2020 AHA/ACC Guideline for the Diagnosis and Treatment of Patients With Hypertrophic Cardiomyopathy: A Report of the American College of Cardiology/American Heart Association Joint Committee on Clinical Practice Guidelines. Journal of the American College of Cardiology. 2020; 76: e159–e240.

[9] Marian AJ, Braunwald E. Hypertrophic Cardiomyopathy: Genetics, Pathogenesis, Clinical Manifestations, Diagnosis, and Therapy. Circulation Research. 2017; 121: 749–770.

[10] Bruder O, Wagner A, Jensen CJ, Schneider S, Ong P, Kispert E, *et al*. Myocardial scar visualized by cardiovascular magnetic resonance imaging predicts major adverse events in patients with hypertrophic cardiomyopathy. Journal of the American College of Cardiology. 2010; 56: 875–887.

[11] To ACY, Dhillon A, Desai MY. Cardiac magnetic resonance in hypertrophic cardiomyopathy. JACC: Cardiovascular Imaging. 2011; 4: 1123–1137.

[12] Maron MS, Hauser TH, Dubrow E, Horst TA, Kissinger KV, Udelson JE, *et al*. Right ventricular involvement in hypertrophic cardiomyopathy. The American Journal of Cardiology. 2007; 100: 1293–1298.

[13] Maron MS, Maron BJ, Harrigan C, Buros J, Gibson CM, Oliv-

otto I, *et al*. Hypertrophic Cardiomyopathy Phenotype Revisited after 50 Years with Cardiovascular Magnetic Resonance. Journal of the American College of Cardiology. 2009; 54: 220–228.
[14] Maron MS, Rowin EJ, Maron BJ. How to Image Hypertrophic Cardiomyopathy. Circulation: Cardiovascular Imaging. 2017; 10: 1–15.
[15] Baxi AJ, Restrepo CS, Vargas D, Marmol-Velez A, Ocazionez D, Murillo H. Hypertrophic Cardiomyopathy from a to Z: Genetics, Pathophysiology, Imaging, and Management. Radiographics. 2016; 36: 335–354.
[16] Olivotto I, Maron MS, Autore C, Lesser JR, Rega L, Casolo G, *et al*. Assessment and Significance of Left Ventricular Mass by Cardiovascular Magnetic Resonance in Hypertrophic Cardiomyopathy. Journal of the American College of Cardiology. 2008; 52: 559–566.
[17] Rowin EJ, Maron BJ, Romashko M, Wang W, Rastegar H, Link MS, *et al*. Impact of Effective Management Strategies on Patients with the most Extreme Phenotypic Expression of Hypertrophic Cardiomyopathy. The American Journal of Cardiology. 2019; 124: 113–121.
[18] Ramchand J, Fava AM, Chetrit M, Desai MY. Advanced imaging for risk stratification of sudden death in hypertrophic cardiomyopathy. Heart. 2019; 106: 1111.2–111112.
[19] Noureldin RA, Liu S, Nacif MS, Judge DP, Halushka MK, Abraham TP, *et al*. The diagnosis of hypertrophic cardiomyopathy by cardiovascular magnetic resonance. Journal of Cardiovascular Magnetic Resonance. 2012; 14: 17.
[20] Masci PG, Dymarkowski S, Bogaert J. Valvular heart disease: what does cardiovascular MRI add? European Radiology. 2008; 18: 197–208.
[21] Rodrigues JCL, Rohan S, Ghosh Dastidar A, Harries I, Lawton CB, Ratcliffe LE, *et al*. Hypertensive heart disease versus hypertrophic cardiomyopathy: multi-parametric cardiovascular magnetic resonance discriminators when end-diastolic wall thickness $\geq$ 15 mm. European Radiology. 2017; 27: 1125–1135.
[22] Hinojar R, Varma N, Child N, Goodman B, Jabbour A, Yu C, *et al*. T1 Mapping in Discrimination of Hypertrophic Phenotypes: Hypertensive Heart Disease and Hypertrophic Cardiomyopathy: Findings from the International T1 Multicenter Cardiovascular Magnetic Resonance Study. Circulation. Cardiovascular Imaging. 2015; 8: 1541–1549.
[23] Maron MS, Finley JJ, Bos JM, Hauser TH, Manning WJ, Haas TS, *et al*. Prevalence, Clinical Significance, and Natural History of Left Ventricular Apical Aneurysms in Hypertrophic Cardiomyopathy. Circulation. 2008; 118: 1541–1549.
[24] Rowin EJ, Maron BJ, Haas TS, Garberich RF, Wang W, Link MS, *et al*. Hypertrophic Cardiomyopathy with Left Ventricular Apical Aneurysm: Implications for Risk Stratification and Management. Journal of the American College of Cardiology. 2017; 69: 761–773.
[25] Takasugi J, Yamagami H, Noguchi T, Morita Y, Tanaka T, Okuno Y, *et al*. Detection of Left Ventricular Thrombus by Cardiac Magnetic Resonance in Embolic Stroke of Undetermined Source. Stroke. 2017; 48: 2434–2440.
[26] Hughes RK, Knott KD, Malcolmson J, Augusto JB, Mohiddin SA, Kellman P, *et al*. Apical Hypertrophic Cardiomyopathy: the Variant less Known. Journal of the American Heart Association. 2020; 9: 1–11.
[27] Berger SG, Sjaastad I, Stokke MK. Right ventricular involvement in hypertrophic cardiomyopathy: evidence and implications from current literature. Scandinavian Cardiovascular Journal. 2021; 55: 195–204.
[28] Elliott PM, Anastasakis A, Borger MA, Borggrefe M, Cecchi F, Charron P, *et al*. 2014 ESC Guidelines on diagnosis and management of hypertrophic cardiomyopathy: the Task Force for the Diagnosis and Management of Hypertrophic Cardiomyopathy of the European Society of Cardiology (ESC). European Heart Journal. 2014; 35: 2733–2779.
[29] Maron MS, Rowin EJ, Lin D, Appelbaum E, Chan RH, Gibson CM, *et al*. Prevalence and Clinical Profile of Myocardial Crypts in Hypertrophic Cardiomyopathy. Circulation: Cardiovascular Imaging. 2012; 5: 441–447.
[30] Sigvardsen PE, Pham MHC, Kühl JT, Fuchs A, Afzal S, Møgelvang R, *et al*. Left ventricular myocardial crypts: morphological patterns and prognostic implications. European Heart Journal - Cardiovascular Imaging. 2021; 22: 75–81.
[31] Musumeci B, Tini G, Russo D, Sclafani M, Cava F, Tropea A, *et al*. Left ventricular remodeling in hypertrophic cardiomyopathy: An overview of current knowledge. Journal of Clinical Medicine. 2021; 10: 1547.
[32] Maron MS, Olivotto I, Zenovich AG, Link MS, Pandian NG, Kuvin JT, *et al*. Hypertrophic cardiomyopathy is predominantly a disease of left ventricular outflow tract obstruction. Circulation. 2006; 114: 2232–2239.
[33] Maron MS, Olivotto I, Harrigan C, Appelbaum E, Gibson CM, Lesser JR, *et al*. Mitral Valve Abnormalities Identified by Cardiovascular Magnetic Resonance Represent a Primary Phenotypic Expression of Hypertrophic Cardiomyopathy. Circulation. 2011; 124: 40–47.
[34] Patel P, Dhillon A, Popovic ZB, Smedira NG, Rizzo J, Thamilarasan M, *et al*. Left Ventricular Outflow Tract Obstruction in Hypertrophic Cardiomyopathy Patients without Severe Septal Hypertrophy: Implications of Mitral Valve and Papillary Muscle Abnormalities Assessed Using Cardiac Magnetic Resonance and Echocardiography. Circulation. Cardiovascular Imaging. 2015; 8: e003132.
[35] Sherrid MV, Balaram S, Kim B, Axel L, Swistel DG. The Mitral Valve in Obstructive Hypertrophic Cardiomyopathy: a Test in Context. Journal of the American College of Cardiology. 2016; 67: 1846–1858.
[36] Maron BJ, Maron MS, Wigle ED, Braunwald E. The 50-Year History, Controversy, and Clinical Implications of Left Ventricular Outflow Tract Obstruction in Hypertrophic Cardiomyopathy. Journal of the American College of Cardiology. 2009; 54: 191–200.
[37] Kwon DH, Setser RM, Thamilarasan M, Popovic ZV, Smedira NG, Schoenhagen P, *et al*. Abnormal papillary muscle morphology is independently associated with increased left ventricular outflow tract obstruction in hypertrophic cardiomyopathy. Heart. 2008; 94: 1295–1301.
[38] Kwon DH, Smedira NG, Thamilarasan M, Lytle BW, Lever H, Desai MY. Characteristics and surgical outcomes of symptomatic patients with hypertrophic cardiomyopathy with abnormal papillary muscle morphology undergoing papillary muscle reorientation. The Journal of Thoracic and Cardiovascular Surgery. 2010; 140: 317–324.
[39] Puntmann VO, Valbuena S, Hinojar R, Petersen SE, Greenwood JP, Kramer CM, *et al*. Society for Cardiovascular Magnetic Resonance (SCMR) expert consensus for CMR imaging endpoints in clinical research: part i - analytical validation and clinical qualification. Journal of Cardiovascular Magnetic Resonance. 2018; 20: 67.
[40] Mewton N, Liu CY, Croisille P, Bluemke D, Lima JAC. Assessment of myocardial fibrosis with cardiovascular magnetic resonance. Journal of the American College of Cardiology. 2011; 57: 891–903.
[41] Gupta S, Ge Y, Singh A, Gräni C, Kwong RY. Multimodality Imaging Assessment of Myocardial Fibrosis. JACC: Cardiovascular Imaging. 2021; 14: 2457–2469.
[42] Green JJ, Berger JS, Kramer CM, Salerno M. Prognostic value of late gadolinium enhancement in clinical outcomes for hypertrophic cardiomyopathy. JACC: Cardiovascular Imaging. 2012;

5: 370–377.
[43] Mentias A, Raeisi-Giglou P, Smedira NG, Feng K, Sato K, Wazni O, *et al*. Late Gadolinium Enhancement in Patients with Hypertrophic Cardiomyopathy and Preserved Systolic Function. Journal of the American College of Cardiology. 2018; 72: 857–870.
[44] Weng Z, Yao J, Chan RH, He J, Yang X, Zhou Y, *et al*. Prognostic Value of LGE-CMR in HCM: A Meta-Analysis. JACC: Cardiovascular Imaging. 2016; 9: 1392–1402.
[45] Weissler-Snir A, Hindieh W, Spears DA, Adler A, Rakowski H, Chan RH. The relationship between the quantitative extent of late gadolinium enhancement and burden of nonsustained ventricular tachycardia in hypertrophic cardiomyopathy: a delayed contrast-enhanced magnetic resonance study. Journal of Cardiovascular Electrophysiology. 2019; 30: 651–657.
[46] Chan RH, Maron BJ, Olivotto I, Pencina MJ, Assenza GE, Haas T, *et al*. Prognostic value of quantitative contrast-enhanced cardiovascular magnetic resonance for the evaluation of sudden death risk in patients with hypertrophic cardiomyopathy. Circulation. 2014; 130: 484–495.
[47] Chan RH, Maron BJ, Olivotto I, Assenza GE, Haas TS, Lesser JR, *et al*. Significance of Late Gadolinium Enhancement at Right Ventricular Attachment to Ventricular Septum in Patients with Hypertrophic Cardiomyopathy. The American Journal of Cardiology. 2015; 116: 436–441.
[48] Ali ND, Behairy N, Kharabish A, Elmozy W, Hegab AY, Saraya S. Cardiac MRI T1 mapping and extracellular volume application in hypertrophic cardiomyopathy. Egyptian Journal of Radiology and Nuclear Medicine. 2021; 52: 58.
[49] Xu J, Zhuang B, Sirajuddin A, Li S, Huang J, Yin G, *et al*. MRI T1 Mapping in Hypertrophic Cardiomyopathy: Evaluation in Patients without Late Gadolinium Enhancement and Hemodynamic Obstruction. Radiology. 2020; 294: 275–286.
[50] Baggiano A, Del Torto A, Guglielmo M, Muscogiuri G, Fusini L, Babbaro M, *et al*. Role of CMR mapping techniques in cardiac hypertrophic phenotype. Diagnostics. 2020; 10: 1–20.
[51] Huang L, Ran L, Zhao P, Tang D, Han R, Ai T, *et al*. MRI native T1 and T2 mapping of myocardial segments in hypertrophic cardiomyopathy: tissue remodeling manifested prior to structure changes. The British Journal of Radiology. 2019; 92: 20190634.
[52] Maron BJ, Casey SA, Chan RH, Garberich RF, Rowin EJ, Maron MS. Independent Assessment of the European Society of Cardiology Sudden Death Risk Model for Hypertrophic Cardiomyopathy. The American Journal of Cardiology. 2015; 116: 757–764.
[53] Vriesendorp PA, Schinkel AFL, Liebregts M, Theuns DAMJ, van Cleemput J, Ten Cate FJ, *et al*. Validation of the 2014 European Society of Cardiology guidelines risk prediction model for the primary prevention of sudden cardiac death in hypertrophic cardiomyopathy. Circulation. Arrhythmia and Electrophysiology. 2015; 8: 829–835.
[54] Klem I, Weinsaft JW, Bahnson TD, Hegland D, Kim HW, Hayes B, *et al*. Assessment of myocardial scarring improves risk stratification in patients evaluated for cardiac defibrillator implantation. Journal of the American College of Cardiology. 2012; 60: 408–420.
[55] Kariki O, Antoniou CK, Mavrogeni S, Gatzoulis KA. Updating the risk stratification for sudden cardiac death in cardiomyopathies: The evolving role of cardiac magnetic resonance imaging. An approach for the electrophysiologist. Diagnostics. 2020; 10: 541.
[56] Goïorani F, Dagrenat C, Brocchi J, Couppie P, Leddet P. Diagnosing cardiac amyloidosis in magnetic resonance imaging: The discriminating factors. Annales de Cardiologie et d Angéiologie. 2020; 69: 262–267.
[57] Martinez-Naharro A, Kotecha T, Norrington K, Boldrini M, Rezk T, Quarta C, *et al*. Native T1 and Extracellular Volume in Transthyretin Amyloidosis. JACC: Cardiovascular Imaging. 2019; 12: 810–819.
[58] Rapezzi C, Merlini G, Quarta CC, Riva L, Longhi S, Leone O, *et al*. Systemic Cardiac Amyloidoses: Disease profiles and clinical courses of the 3 main types. Circulation. 2009; 120: 1203–1212.
[59] Falk RH, Kruger J, Cristina Quarta C. Senile systemic amyloidosis is a markedly underdiagnosed cardiomyopathy: experience of a cardiac amyloidosis program. Journal of the American College of Cardiology. 2013; 61: E1241.
[60] Aimo A, Emdin M, Barison A. Magnetic Resonance to Diagnose Cardiac Amyloidosis. JACC: Cardiovascular Imaging. 2020; 13: 1293–1294.
[61] Dorbala S, Cuddy S, Falk RH. How to Image Cardiac Amyloidosis. JACC: Cardiovascular Imaging. 2020; 13: 1368–1383.
[62] Banypersad SM, Sado DM, Flett AS, Gibbs SDJ, Pinney JH, Maestrini V, *et al*. Quantification of myocardial extracellular volume fraction in systemic AL amyloidosis: an equilibrium contrast cardiovascular magnetic resonance study. Circulation. Cardiovascular Imaging. 2013; 6: 34–39.
[63] Karamitsos TD, Piechnik SK, Banypersad SM, Fontana M, Ntusi NB, Ferreira VM, *et al*. Noncontrast T1 mapping for the diagnosis of cardiac amyloidosis. JACC: Cardiovascular Imaging. 2013; 6: 488–497.
[64] Fontana M, Banypersad SM, Treibel TA, Maestrini V, Sado DM, White SK, *et al*. Native T1 Mapping in Transthyretin Amyloidosis. JACC: Cardiovascular Imaging. 2014; 7: 157–165.
[65] Tuzovic M, Yang EH, Baas AS, Depasquale EC, Deng MC, Cruz D, *et al*. Cardiac Amyloidosis: Diagnosis and Treatment Strategies. Current Oncology Reports. 2017; 19: 46.
[66] Tang CX, Petersen SE, Sanghvi MM, Lu GM, Zhang LJ. Cardiovascular magnetic resonance imaging for amyloidosis: the state-of-the-art. Trends in Cardiovascular Medicine. 2019; 29: 83–94.
[67] Martinez-Naharro A, Treibel TA, Abdel-Gadir A, Bulluck H, Zumbo G, Knight DS, *et al*. Magnetic Resonance in Transthyretin Cardiac Amyloidosis. Journal of the American College of Cardiology. 2017; 70: 466–477.
[68] Gertz MA, Benson MD, Dyck PJ, Grogan M, Coelho T, Cruz M, *et al*. Diagnosis, Prognosis, and Therapy of Transthyretin Amyloidosis. Journal of the American College of Cardiology. 2015; 66: 2451–2466.
[69] Siddiqi OK, Ruberg FL. Challenging the myths of cardiac amyloidosis. European Heart Journal. 2017; 38: 1909–1912.
[70] Rehwald WG, Fieno DS, Chen E, Kim RJ, Judd RM. Myocardial magnetic resonance imaging contrast agent concentrations after reversible and irreversible ischemic injury. Circulation. 2002; 105: 224–229.
[71] Zhao L, Tian Z, Fang Q. Diagnostic accuracy of cardiovascular magnetic resonance for patients with suspected cardiac amyloidosis: a systematic review and meta-analysis. BMC Cardiovascular Disorders. 2016; 16: 129.
[72] Maceira AM, Joshi J, Prasad SK, Moon JC, Perugini E, Harding I, *et al*. Cardiovascular magnetic resonance in cardiac amyloidosis. Circulation. 2005; 111: 186–193.
[73] Syed IS, Glockner JF, Feng D, Araoz PA, Martinez MW, Edwards WD, *et al*. Role of Cardiac Magnetic Resonance Imaging in the Detection of Cardiac Amyloidosis. JACC: Cardiovascular Imaging. 2010; 3: 155–164.
[74] Fontana M, Pica S, Reant P, Abdel-Gadir A, Treibel TA, Banypersad SM, *et al*. Prognostic Value of Late Gadolinium Enhancement Cardiovascular Magnetic Resonance in Cardiac Amyloidosis. Circulation. 2015; 132: 1570–1579.
[75] Yilmaz A, Bauersachs J, Bengel F, Büchel R, Kindermann I, Klingel K, *et al*. Diagnosis and treatment of cardiac amyloidosis: position statement of the German Cardiac Society (DGK).

Clinical Research in Cardiology. 2021; 110: 479–506.
[76] Chacko L, Martone R, Cappelli F, Fontana M. Cardiac Amyloidosis: Updates in Imaging. Current Cardiology Reports. 2019; 21: 108.
[77] Muellerleile K, Lund GK. Cardiovascular Magnetic Resonance in Cardiac Amyloidosis: T1 is not enough. Journal of the American College of Cardiology. 2018; 71: 2932–2934.
[78] Baggiano A, Boldrini M, Martinez-Naharro A, Kotecha T, Petrie A, Rezk T, *et al*. Noncontrast Magnetic Resonance for the Diagnosis of Cardiac Amyloidosis. JACC: Cardiovascular Imaging. 2020; 13: 69–80.
[79] Manning WJ, Pennell DJ. Cardiovascular Magnetic Resonance: A companion to Brauwnwald's Heart Disease. 3rd edn. Elsevier: Philadelphia, PA. 2019.
[80] Coelho-Filho OR, Shah RV, Mitchell R, Neilan TG, Moreno H, Simonson B, *et al*. Quantification of Cardiomyocyte Hypertrophy by Cardiac Magnetic Resonance. Circulation. 2013; 128: 1225–1233.
[81] Kotecha T, Martinez-Naharro A, Treibel TA, Francis R, Nordin S, Abdel-Gadir A, *et al*. Myocardial Edema and Prognosis in Amyloidosis. Journal of the American College of Cardiology. 2018; 71: 2919–2931.
[82] Brissot P, Loréal O. Iron metabolism and related genetic diseases: a cleared land, keeping mysteries. Journal of Hepatology. 2016; 64: 505–515.
[83] Bozkurt B, Colvin M, Cook J, Cooper LT, Deswal A, Fonarow GC, *et al*. Current Diagnostic and Treatment Strategies for Specific Dilated Cardiomyopathies: a Scientific Statement from the American Heart Association. Circulation. 2016; 134: e579–e646.
[84] Kremastinos DT, Farmakis D. Iron overload cardiomyopathy in clinical practice. Circulation. 2011; 124: 2253–2263.
[85] Meloni A, Martini N, Positano V, De Luca A, Pistoia L, Sbragi S, *et al*. Myocardial iron overload by cardiovascular magnetic resonance native segmental T1 mapping: a sensitive approach that correlates with cardiac complications. Journal of Cardiovascular Magnetic Resonance. 2021; 23: 70.
[86] Wood JC. Guidelines for quantifying iron overload. Hematology. 2014; 2014: 210–215.
[87] Pereira NL, Grogan M, Dec GW. Spectrum of Restrictive and Infiltrative Cardiomyopathies: Part 2 of a 2-Part Series. Journal of the American College of Cardiology. 2018; 71: 1149–1166.
[88] Murphy CJ, Oudit GY. Iron-overload cardiomyopathy: pathophysiology, diagnosis, and treatment. Journal of Cardiac Failure. 2010; 16: 888–900.
[89] Wood JC, Otto-Duessel M, Aguilar M, Nick H, Nelson MD, Coates TD, *et al*. Cardiac iron determines cardiac T2*, T2, and T1 in the gerbil model of iron cardiomyopathy. Circulation. 2005; 112: 535–543.
[90] Labranche R, Gilbert G, Cerny M, Vu K, Soulières D, Olivié D, *et al*. Liver Iron Quantification with MR Imaging: a Primer for Radiologists. Radiographics. 2018; 38: 392–412.
[91] Anderson LJ, Holden S, Davis B, Prescott E, Charrier CC, Bunce NH, *et al*. Cardiovascular T2-star (T2*) magnetic resonance for the early diagnosis of myocardial iron overload. European Heart Journal. 2001; 22: 2171–2179.
[92] Pepe A, Positano V, Santarelli MF, Sorrentino F, Cracolici E, De Marchi D, *et al*. Multislice multiecho T2* cardiovascular magnetic resonance for detection of the heterogeneous distribution of myocardial iron overload. Journal of Magnetic Resonance Imaging. 2006; 23: 662–668.
[93] Meloni A, Restaino G, Borsellino Z, Caruso V, Spasiano A, Zuccarelli A, *et al*. Different patterns of myocardial iron distribution by whole-heart T2* magnetic resonance as risk markers for heart complications in thalassemia major. International Journal of Cardiology. 2014; 177: 1012–1019.
[94] Kirk P, Roughton M, Porter JB, Walker JM, Tanner MA, Patel J, *et al*. Cardiac T2* Magnetic Resonance for Prediction of Cardiac Complications in Thalassemia Major. Circulation. 2009; 120: 1961–1968.
[95] Modell B, Khan M, Darlison M, Westwood MA, Ingram D, Pennell DJ. Improved survival of thalassaemia major in the UK and relation to T2* cardiovascular magnetic resonance. Journal of Cardiovascular Magnetic Resonance. 2008; 10: 42.
[96] Germain DP. Fabry disease. Orphanet Journal of Rare Diseases. 2010; 5: 30.
[97] Ioannou YA, Zeidner KM, Gordon RE, Desnick RJ. Fabry Disease: Preclinical Studies Demonstrate the Effectiveness of $\alpha$-Galactosidase a Replacement in Enzyme-Deficient Mice. The American Journal of Human Genetics. 2001; 68: 14–25.
[98] Waldek S, Patel MR, Banikazemi M, Lemay R, Lee P. Life expectancy and cause of death in males and females with Fabry disease: Findings from the Fabry Registry. Genetics in Medicine. 2009; 11: 790–796.
[99] Serra W, Marziliano N. Role of cardiac imaging in Anderson-Fabry cardiomyopathy. Cardiovascular Ultrasound. 2019; 17: 1.
[100] Hughes DA, Elliott PM, Shah J, Zuckerman J, Coghlan G, Brookes J, *et al*. Effects of enzyme replacement therapy on the cardiomyopathy of Anderson-Fabry disease: a randomised, double-blind, placebo-controlled clinical trial of agalsidase alfa. Heart. 2008; 94: 153–158.
[101] Elliott P, Baker R, Pasquale F, Quarta G, Ebrahim H, Mehta AB, *et al*. Prevalence of Anderson-Fabry disease in patients with hypertrophic cardiomyopathy: the European Anderson-Fabry Disease survey. Heart. 2011; 97: 1957–1960.
[102] Deva DP, Hanneman K, Li Q, Ng MY, Wasim S, Morel C, *et al*. Cardiovascular magnetic resonance demonstration of the spectrum of morphological phenotypes and patterns of myocardial scarring in Anderson-Fabry disease. Journal of Cardiovascular Magnetic Resonance. 2016; 18: 14.
[103] Tower-Rader A, Jaber WA. Multimodality Imaging Assessment of Fabry Disease. Circulation: Cardiovascular Imaging. 2019; 12: 1–13.
[104] Hazari H, Belenkie I, Kryski A, White JA, Oudit GY, Thompson R, *et al*. Comparison of Cardiac Magnetic Resonance Imaging and Echocardiography in Assessment of Left Ventricular Hypertrophy in Fabry Disease. The Canadian Journal of Cardiology. 2018; 34: 1041–1047.
[105] Moon JCC, Sachdev B, Elkington AG, McKenna WJ, Mehta A, Pennell DJ, *et al*. Gadolinium enhanced cardiovascular magnetic resonance in Anderson-Fabry disease. Evidence for a disease specific abnormality of the myocardial interstitium. European Heart Journal. 2003; 24: 2151–2155.
[106] Sado DM, Flett AS, Banypersad SM, White SK, Maestrini V, Quarta G, *et al*. Cardiovascular magnetic resonance measurement of myocardial extracellular volume in health and disease. Heart. 2012; 98: 1436–1441.
[107] Hanneman K, Karur GR, Wasim S, Morel CF, Iwanochko RM. Prognostic Significance of Cardiac Magnetic Resonance Imaging Late Gadolinium Enhancement in Fabry Disease. Circulation. 2018; 138: 2579–2581.
[108] Sado DM, White SK, Piechnik SK, Banypersad SM, Treibel T, Captur G, *et al*. Identification and assessment of Anderson-Fabry disease by cardiovascular magnetic resonance noncontrast myocardial T1 mapping. Circulation. Cardiovascular Imaging. 2013; 6: 392–398.
[109] Thompson RB, Chow K, Khan A, Chan A, Shanks M, Paterson I, *et al*. T1 mapping with cardiovascular MRI is highly sensitive for fabry disease independent of hypertrophy and sex. Circulation: Cardiovascular Imaging. 2013; 6: 637–645.
[110] Weidemann F, Niemann M, Breunig F, Herrmann S, Beer M, Störk S, *et al*. Long-term effects of enzyme replacement therapy

on fabry cardiomyopathy: evidence for a better outcome with early treatment. Circulation. 2009; 119: 524–529.

[111] Corrado D, Van Tintelen PJ, McKenna WJ, Hauer RNW, Anastastakis A, Asimaki A, et al. Arrhythmogenic right ventricular cardiomyopathy: Evaluation of the current diagnostic criteria and differential diagnosis. European Heart Journal. 2020; 41: 1414–1427b.

[112] te Riele ASJM, Tandri H, Bluemke DA. Arrhythmogenic right ventricular cardiomyopathy (ARVC): cardiovascular magnetic resonance update. Journal of Cardiovascular Magnetic Resonance. 2014; 16: 50.

[113] Marcus FI, McKenna WJ, Sherrill D, Basso C, Bauce B, Bluemke DA, *et al.* Diagnosis of arrhythmogenic right ventricular cardiomyopathy/dysplasia. European Heart Journal. 2010; 31: 806–814.

[114] Perazzolo Marra M, Rizzo S, Bauce B, De Lazzari M, Pilichou K, Corrado D, *et al*. Arrhythmogene rechtsventrikuläre Kardiomyopathie: Beitrag der kardialen Magnetresonanztomographie bei der Diagnosestellung. Herz. 2015; 40: 600–606.

[115] Galea N, Carbone I, Cannata D, Cannavale G, Conti B, Galea R, *et al*. Right ventricular cardiovascular magnetic resonance imaging: normal anatomy and spectrum of pathological findings. Insights into Imaging. 2013; 4: 213–223.

[116] Te Riele ASJM, James CA, Philips B, Rastegar N, Bhonsale A, Groeneweg JA, *et al*. Mutation-positive arrhythmogenic right ventricular dysplasia/cardiomyopathy: the triangle of dysplasia displaced. Journal of Cardiovascular Electrophysiology. 2013; 24: 1311–1320.

[117] Etoom Y, Govindapillai S, Hamilton R, Manlhiot C, Yoo S, Farhan M, *et al*. Importance of CMR within the Task Force Criteria for the diagnosis of ARVC in children and adolescents. Journal of the American College of Cardiology. 2015; 65: 987–995.

[118] Gandjbakhch E, Redheuil A, Pousset F, Charron P, Frank R. Clinical Diagnosis, Imaging, and Genetics of Arrhythmogenic Right Ventricular Cardiomyopathy/Dysplasia: JACC State-of-the-Art Review. Journal of the American College of Cardiology. 2018; 72: 784–804.

[119] Bourfiss M, Vigneault DM, Aliyari Ghasebeh M, Murray B, James CA, Tichnell C, *et al*. Feature tracking CMR reveals abnormal strain in preclinical arrhythmogenic right ventricular dysplasia/cardiomyopathy: a multisoftware feasibility and clinical implementation study. Journal of Cardiovascular Magnetic Resonance. 2017; 19: 66.

[120] Tandri H, Castillo E, Ferrari VA, Nasir K, Dalal D, Bomma C, *et al*. Magnetic resonance imaging of arrhythmogenic right ventricular dysplasia: sensitivity, specificity, and observer variability of fat detection versus functional analysis of the right ventricle. Journal of the American College of Cardiology. 2006; 48: 2277–2284.

[121] Tandri H, Calkins H, Nasir K, Bomma C, Castillo E, Rutberg J, *et al*. Magnetic resonance imaging findings in patients meeting task force criteria for arrhythmogenic right ventricular dysplasia. Journal of Cardiovascular Electrophysiology. 2003; 14: 476–482.

[122] Aquaro GD, Barison A, Todiere G, Grigoratos C, Ait Ali L, Di Bella G, *et al*. Usefulness of Combined Functional Assessment by Cardiac Magnetic Resonance and Tissue Characterization Versus Task Force Criteria for Diagnosis of Arrhythmogenic Right Ventricular Cardiomyopathy. The American Journal of Cardiology. 2016; 118: 1730–1736.

[123] Deac M, Alpendurada F, Fanaie F, Vimal R, Carpenter J, Dawson A, *et al*. Prognostic value of cardiovascular magnetic resonance in patients with suspected arrhythmogenic right ventricular cardiomyopathy. International Journal of Cardiology. 2013; 168: 3514–3521.

[124] Ruberg FL, Grogan M, Hanna M, Kelly JW, Maurer MS. Transthyretin Amyloid Cardiomyopathy: JACC State-of-the-Art Review. Journal of the American College of Cardiology. 2019; 73: 2872–2891.